Metabolic Engineering 61 (2020) 171–180

Contents lists available at ScienceDirect

Metabolic Engineering

journal homepage: www.elsevier.com/locate/meteng

Original Research Article

Engineered citrate synthase alters Acetate Accumulation in *Escherichia coli*

D. Brisbane Tovilla-Coutiño [a], Cory Momany [b], Mark A. Eiteman [a,*]

[a] School of Chemical, Materials and Biomedical Engineering, University of Georgia, Athens, GA, 30602, USA
[b] Dept. of Pharmaceutical and Biomedical Sciences, University of Georgia, Athens, GA, 30602, USA

ARTICLE INFO

Keywords:
Acetyl-CoA
Batch culture
Chemostat
Citrate synthase variants
Point mutations

ABSTRACT

Metabolic engineering is used to improve titers, yields and generation rates for biochemical products in host microbes such as *Escherichia coli*. A wide range of biochemicals are derived from the central carbon metabolite acetyl-CoA, and the largest native drain of acetyl-CoA in most microbes including *E. coli* is entry into the tricarboxylic acid (TCA) cycle via citrate synthase (coded by the *gltA* gene). Since the pathway to any biochemical derived from acetyl-CoA must ultimately compete with citrate synthase, a reduction in citrate synthase activity should facilitate the increased formation of products derived from acetyl-CoA. To test this hypothesis, we integrated into *E. coli* C Δ*poxB* twenty-eight citrate synthase variants having specific point mutations that were anticipated to reduce citrate synthase activity. These variants were assessed in shake flasks for growth and the production of acetate, a model product derived from acetyl-CoA. Mutations in citrate synthase at residues W260, A267 and V361 resulted in the greatest acetate yields (approximately 0.24 g/g glucose) compared to the native citrate synthase (0.05 g/g). These variants were further examined in controlled batch and continuous processes. The results provide important insights on improving the production of compounds derived from acetyl-CoA.

1. Introduction

Microbially-derived biochemicals are generated using living cells in fermentation processes as an alternative to traditional petrochemical-based processes. Acetyl-CoA is a key metabolic precursor for many biochemicals of industrial interest such as 1-butanol, fatty acids, polyhydroxyalkanoates, polyketides and isoprenoids (Krivoruchko et al., 2015). Acetyl-CoA bridges the Embden-Meyerhof-Parnas (EMP) pathway and the tricarboxylic acid cycle (TCA cycle, Fig. 1). Biosynthetic fluxes and numerous cell functions are regulated by acetyl-CoA (Fuchs and Berg, 2014; Pontrelli et al., 2018), and this metabolite influences the activity of many enzymes, either in an allosteric manner or by altering substrate availability (Pietrocola et al., 2015). Consequently, there has been much interest in engineering central metabolism with the goal of increasing acetyl-CoA availability to ensure that adequate levels of this precursor are available for the synthesis of target products derived from acetyl-CoA.

Several studies have aimed to increase the production of biochemicals derived from acetyl-CoA based on the metabolic engineering of pathways that consume or produce acetyl-CoA. For example, production of n-butanol in *Escherichia coli* achieved 5.4-fold greater yields using an artificial transcriptional regulator with clustered regularly interspaced short palindromic repeats interference (CRISPRi) to repress the expression of *pta*, *frdA*, *ldhA*, and *adhE* genes (Kim et al., 2017). Coordinated overexpression of the pyruvate dehydrogenase complex under aerobic conditions increased the acetyl-CoA pool, resulting in an 80% enhanced isoamyl acetate production in a *E. coli* Δ*poxB* Δ*pta* Δ*ackA* strain (Dittrich et al., 2005b). An increase in the expression of acetyl-CoA synthase (*acs* gene) and acetyl-CoA carboxylase (*acc*) increased the formation of pinocembrin from 29 mg/L to 429 mg/L in *E. coli* harboring the flavonoid pathway (Leonard et al., 2007). A heterologous pathway with *phaA* and *phaB* genes from *Ralstonia eutropha* accumulated (R)-3-hydroxybutyrate (R3HB) in *E. coli* using propionyl-CoA transferase (PCT) from *Clostridium propionicum* for the coupled regeneration of acetyl-CoA from acetate (Matsumoto et al., 2013). Because of the PCT equilibrium, the addition of acetate into the medium facilitated the regeneration of acetyl-CoA, leading to a 5.2-fold increase in R3HB. In general, approaches to generate a product include regulation or deletion of competing pathways (Lin et al., 2013; Saini et al., 2016; Kim et al., 2017), modulation of central carbon metabolism (Krivoruchko et al., 2015; Leonard et al., 2007; Dittrich et al., 2005b) and/or introduction of heterologous pathways (Bogorad et al., 2013;

* Corresponding author.
E-mail address: eiteman@engr.uga.edu (M.A. Eiteman).

https://doi.org/10.1016/j.ymben.2020.06.006
Received 24 March 2020; Received in revised form 24 May 2020; Accepted 10 June 2020
Available online 20 June 2020

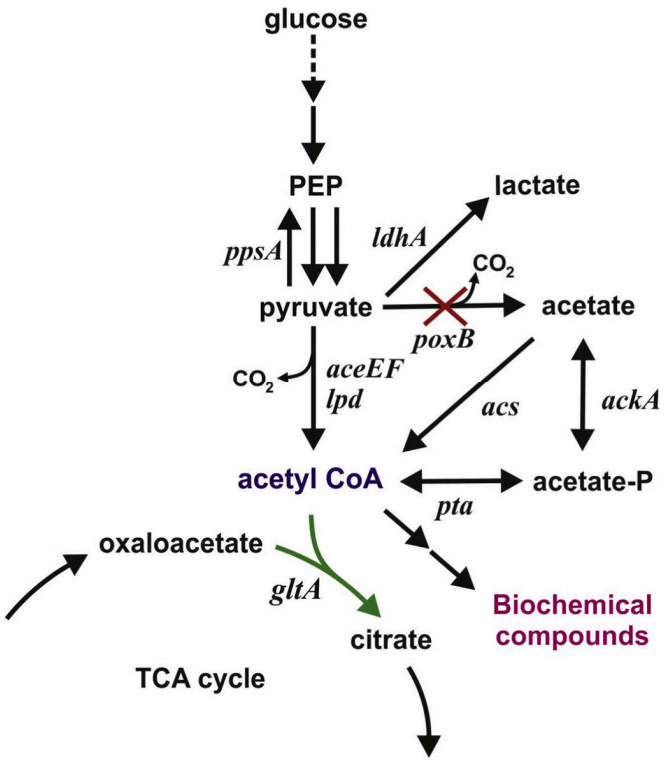

Fig. 1. Metabolic pathways associated with aerobic acetyl-CoA metabolism in *Escherichia coli*. Key genes include: *ppsA* (phosphoenolpyruvate synthetase), *aceEF* and *lpd* (decarboxylase E1, dihydrolipoamide acetyltransferase E2, and lipoamide dehydrogenase components of pyruvate dehydrogenase complex), *ldhA* (lactate dehydrogenase), *pta* (phosphotransacetylase), *ackA* (acetate kinase), *poxB* (pyruvate oxidase), *acs* (acetyl-CoA synthase) and *gltA* (citrate synthase). All *E. coli* C strains examined contained knockouts of the *poxB* gene, and contained different mutations in citrate synthase (green). (For interpretation of the references to colour in this figure legend, the reader is referred to the Web version of this article.)

Matsumoto et al., 2013).

Acetate is generated by endogenous enzymes in *E. coli* and its formation depends on the cellular availability of acetyl-CoA and pyruvate. Acetate is excreted when *E. coli* is growing at a high rate of glucose consumption even under fully aerobic conditions, a complex phenomenon known as overflow metabolism (Eiteman and Altman, 2006; De Mey et al., 2007). In *E. coli* acetate is synthesized primarily by the coordinated activity of phosphotransacetylase (Pta, *pta* gene) and acetate kinase (AckA, *ackA*), or by pyruvate oxidase (*poxB*). Pta catalyzes the reaction of acetyl-CoA with inorganic phosphate to acetyl phosphate (Fig. 1), then AckA converts acetyl phosphate and ADP to acetate and ATP (Dittrich et al., 2005a). Alternately, pyruvate is metabolized to acetate by pyruvate oxidase, a pathway more active during the late growth and stationary phases (De Mey et al., 2007). Pta-AckA contributes both to consumption and generation of acetate and is controlled by the extracellular acetate concentration (Enjalbert et al., 2017). A Δ*poxB* background would ensure that the majority of acetate accumulated by *E. coli* is derived from acetyl-CoA, permitting acetate accumulation to be a direct indicator of the acetyl-CoA pool.

A fundamental constraint in developing microbial processes is the need to balance the carbon flux between native pathways used for cell growth and introduced, non-native pathways to a target product. The introduction of a new pathway in *E. coli* to an acetyl-CoA-derived biochemical, for example, must compete with the activity of native acetyl-CoA-consuming enzymes directed toward the TCA cycle and other biomass precursors including fatty acids (Fig. 1). During aerobic growth of *E. coli* on glucose, the TCA cycle is the primary drain on acetyl-CoA, with more than 62% of the acetyl-CoA flowing through the enzyme citrate synthase (Zhao et al., 2004). Because during typical cell growth the majority of acetyl-CoA enters the TCA cycle, reducing this flux would likely have the most profound effect on the availability of acetyl-CoA for pathways to any acetyl-CoA-derived biochemical. Indeed, reducing citrate synthase (*gltA* gene) expression has been examined previously to alter product formation including modulating promoter strength for L-lysine formation (van Ooyen et al., 2012) and on/off toggling of expression for isopropanol formation (Soma et al., 2014). Another approach to decrease the flux through citrate synthase might be to alter the intrinsic activity of this enzyme (i.e., decrease k_{cat} and/or increase K_M). Some studies on citrate synthase have focused on the function of active site residues and the NADH allosteric binding site (Pereira et al., 1994; Chen et al., 2011). For example, G181E and T204R citrate synthase variants lose sensitivity to NADH (Duckworth et al., 2013). Similarly, GltA[C206S], GltA[E207A] and GltA[C206S; E207A] (both mutations present) bind NADH more weakly than the wild type enzyme (Donald et al., 1991). Mutations in key residues H305, R314, or R387 associated with the oxaloacetate binding pocket essentially eliminate activity (Pereira et al., 1994).

Considering that most of the acetyl-CoA in *E. coli* during growth on glucose flows through citrate synthase, we constructed numerous *E. coli gltA* variants harboring point mutations with the goal of reducing but not eliminating the activity of citrate synthase. We hypothesize that a reduction in citrate synthase activity in *E. coli* Δ*poxB* strains will cause an increase in formation of compounds derived from acetyl-CoA using glucose as the sole carbon source. In this study, acetate itself is used as the model biochemical product derived from acetyl-CoA.

2. Materials and methods

2.1. Strain construction

Strains used in this study are shown in Table 1. The *poxB* and *gltA* knockouts to generate MEC796 and MEC802 were transduced into *E. coli* C using the KEIO collection (Baba et al., 2006) by the P1 phage method, with the kanamycin antibiotic marker removed using the pCP20 plasmid (Datsenko and Wanner, 2000). PCR was used to verify proper chromosomal integration of the kanamycin cassette and the removal of this marker in cured strains.

In order to construct citrate synthase variants, the *gltA* gene from *E. coli* C, a kanamycin cassette from pKD4 (Datsenko and Wanner, 2000) and 500 nt of sequence identical to the target locus upstream and downstream from the *gltA* region of the recipient strain (MEC802), were assembled into the pKSI-1 plasmid (Yang et al., 2014) using the NEBuilder® kit according to manufacturer instructions (New England BioLabs, Ipswich, MA, USA). *E. coli* DH5α was used as a host strain for cloning procedures. The plasmid base (pDBT) served as a template to reintroduce the native *gltA* and generate the variants in plasmids via site-directed mutagenesis with specific primer design. The residues targeted for modification were selected by visual inspection of the citrate synthase atomic structure PDB ID 4G6B (Duckworth et al., 2013) using software for molecular visualization (PyMOL Molecular Graphics System, Schrödinger, Inc. New York, NY). Thirty-one plasmids were constructed including the native *gltA* and the target point mutations. Plasmids and primers used in this study are summarized in Supplemental Material (Tables S1 and S2).

For the integration of the *gltA* variants into the *E. coli* chromosome, each variant with the kanamycin cassette (Kan) from its respective plasmid was amplified with PCR using Phusion® High-Fidelity DNA Polymerase (ThermoFisher Scientific, Walthan, MA, USA). The PCR product was transformed into MEC802 expressing λ Red recombinase proteins encoded on pKD46 (Datsenko and Wanner, 2000). The native and variant *gltA* genes were reconstructed with the adjacent Kan insertion downstream. Gene replacement was selected with kanamycin plates (50 mg/L) and then verified by PCR. In addition, 100 mg/L ampicillin

Table 1
Strains used in this study.

Strain	Genotype	Reference
ATCC 8739	*E. coli C*	ATCC
DH5α	General *E. coli* cloning strain	New England Biolabs
MEC796	ATCC 8739 Δ*poxB*772::(FRT)	This study
MEC802	MEC796 Δ*gltA*770::(FRT)	This study
MEC881	MEC796 Δ*gltA*770::*gltA*[W260P; Kan]	This study
MEC882	MEC796 Δ*gltA*770::*gltA*[Kan]	This study
MEC883	MEC796 Δ*gltA*770::*gltA*[V361I; Kan]	This study
MEC884	MEC796 Δ*gltA*770::*gltA*[V361A; Kan]	This study
MEC885	MEC796 Δ*gltA*770::*gltA*[V361T; Kan]	This study
MEC886	MEC796 Δ*gltA*770::*gltA*[M372S; Kan]	This study
MEC887	MEC796 Δ*gltA*770::*gltA*[M372D; Kan]	This study
MEC888	MEC796 Δ*gltA*770::*gltA*[M372K; Kan]	This study
MEC889	MEC796 Δ*gltA*770::*gltA*[A267L; Kan]	This study
MEC890	MEC796 Δ*gltA*770::*gltA*[A267T; Kan]	This study
MEC891	MEC796 Δ*gltA*770::*gltA*[A267V; Kan]	This study
MEC892	MEC796 Δ*gltA*770::*gltA*[E286D; Kan]	This study
MEC893	MEC796 Δ*gltA*770::*gltA*[S376T; Kan]	This study
MEC894	MEC796 Δ*gltA*770::*gltA*[S376C; Kan]	This study
MEC895	MEC796 Δ*gltA*770::*gltA*[S376H; Kan]	This study
MEC896	MEC796 Δ*gltA*770::*gltA*[W260F; Kan]	This study
MEC897	MEC796 Δ*gltA*770::*gltA*[W260H; Kan]	This study
MEC898	MEC796 Δ*gltA*770::*gltA*[S297K; Kan]	This study
MEC899	MEC796 Δ*gltA*770::*gltA*[S297M; Kan]	This study
MEC900	MEC796 Δ*gltA*770::*gltA*[S297T; Kan]	This study
MEC901	MEC796 Δ*gltA*770::*gltA*[D362V; M372K; Kan]	This study
MEC931	MEC796 Δ*gltA*770::*gltA*[W260V; Kan]	This study
MEC932	MEC796 Δ*gltA*770::*gltA*[V361A; M372S; Kan]	This study
MEC937	MEC796 Δ*gltA*770::*gltA*[V361Q; Kan]	This study
MEC938	MEC796 Δ*gltA*770::*gltA*[W260I; Kan]	This study
MEC939	MEC796 Δ*gltA*770::*gltA*[W260T; Kan]	This study
MEC940	MEC796 Δ*gltA*770::*gltA*[W260F; V361A; Kan]	This study
MEC941	MEC796 Δ*gltA*770::*gltA*[S297M; M372S; Kan]	This study
MEC942	MEC796 Δ*gltA*770::*gltA*[F383M; Kan]	This study

and/or 50 mg/L kanamycin were added for plasmid-containing strains. Plasmid pKD46 was cured at 42 °C. Each *gltA* gene generated in a plasmid and integrated into the chromosome of *E. coli* was sequenced to confirm the correct point mutation (ACGT Inc. Wheeling, IL, USA). The Kan associated with the *gltA* gene remained in the chromosome of the strains.

2.2. Growth medium

Defined medium contained (per L): 3.5 g NH_4Cl, 0.29 g KH_2PO_4, 0.5 g $K_2HPO_4{\cdot}3H_2O$, 2 g K_2SO_4, 20 mg $Na_2(EDTA){\cdot}2H_2O$, 0.45 g $MgSO_4{\cdot}7H_2O$, 0.25 mg $ZnSO_4{\cdot}7H_2O$, 0.125 mg $CuCl_2{\cdot}2H_2O$, 1.25 mg $MnSO_4{\cdot}H_2O$, 0.875 mg $CoCl_2{\cdot}6H_2O$, 0.06 mg H_3BO_3, 0.25 mg $Na_2MoO_4{\cdot}2H_2O$, 5.5 mg $FeSO_4{\cdot}7H_2O$, 20 mg thiamine·HCl, and 20 mg citric acid. Shake flask experiments used this medium with 5.0 g/L glucose and 100 mM of 3-[N-morpholino] propanesulfonic acid (MOPS). Batch experiments in a bioreactor were conducted using identical medium except with (per L) 15.0 g glucose, 4.5 g NH_4Cl, 0.435 g KH_2PO_4, 0.75 g $K_2HPO_4{\cdot}3H_2O$, 100 mg citric acid (and no MOPS). Steady-state chemostat experiments used the same medium as batch experiments except 100 mM MOPS and 25 g/L glucose, 0.5 g/L NH_4Cl (for nitrogen-limited chemostat) or 8.0 g/L glucose and 4.5 g/L NH_4Cl (for carbon-limited chemostat).

2.3. Shake flask, batch and steady-state processes

Shake flask experiments examined the effect of each *gltA* variant on growth rate and acetate formation in *E. coli* Δ*poxB*. Cells were first grown in 3 mL Lysogeny Broth (LB) in 16 × 150 mm test tubes at 37 °C and 250 rpm. After 6–10 h, a 100 × dilution was used to inoculate 4 mL of defined medium in 16 × 150 mm test tubes. After 10–15 h, 0.5–1 mL of this second culture was used to inoculate in triplicate 50 mL medium in 250 mL baffled shake flasks, which were then cultured at 37 °C and 250 rpm for 10–24 h until glucose was depleted. Samples were withdrawn periodically from each culture to determine growth rate, glucose, and acetate concentration.

Batch processes were conducted in duplicate in a 2.5 L bioreactor (Bioflo 2000; New Brunswick Scientific Co. New Brunswick, NJ) with 1.0 L as operating volume. Cells were first grown as described above for shake flasks, and when the shake flask culture reached an optical density (OD) of 1.5–2.0, the 50 mL contents were used to inoculate the bioreactor. The agitation was set at 350 rpm, and air was sparged at 1.0 L/min. When necessary, oxygen was added to maintain the dissolved oxygen above 40% of saturation. The pH was controlled at 7.0 using 30% (w/v) KOH, and the temperature was maintained at 37 °C.

Continuous processes operated as a chemostat were conducted in a 0.5 L volume and initiated in batch mode in a 1.0 L bioreactor (Bioflo 310, New Brunswick Scientific Co. New Brunswick, NJ, USA). The culture medium was continuously fed to and withdrawn from the bioreactor (nitrogen-limited chemostat used a dilution rate (D) of 0.2 h^{-1}, while carbon-limited chemostat used dilution rates of 0.14–0.30 h^{-1}). The pH was controlled at 7.0 using 30% (w/v) KOH, the temperature at 37 °C, an air flow rate of 0.5 L/min (mixture of O_2 and air), and an agitation of 450 rpm to maintain the DO above 40% saturation. A steady-state condition was attained after a minimum of five residence times. For dry cell weight (DCW) measurement, three 20.0 mL samples were centrifuged (5000×*g*, 10 min), then the pellets were washed three times with 10 mL DI water, centrifuged, and finally the cell pellets dried at 60 °C for 24 h. A yield calculation was based on the mass of the acetate generated divided by the mass of glucose consumed. Statistical analyses were completed using two-sample *t*-Test, and $\alpha = 0.05$ was considered the criterion for significance.

2.4. Analytical methods

The optical density (OD) at 600 nm (DU-650 spectrophotometer, Beckman Instruments, San Jose, CA, USA) was used to monitor cell growth. Approximately 6 samples during exponential growth of the shake flask experiments were used to calculate the specific growth rate. Extracellular glucose and organic acids were analyzed by HPLC using a Refractive Index detector (Eiteman and Chastain, 1997).

2.5. Protein purification

The *gltA* gene sequences from strains MEC882 and MEC890 were PCR amplified using Phusion® High-Fidelity DNA Polymerase. These PCR products were cloned into the pET-28bCH (+) expression vector to create N-terminal His_6 gene fusions (Galloway et al., 2013). The sequences of the *gltA* were confirmed from each plasmid (ACGT Inc. Wheeling, IL, USA), and each *gltA* pET-28bCH (+) plasmid was transformed into *E. coli* BL21(DE3). For protein expression, cultures were grown in 500 mL of autoinduction medium (Studier, 2005) in 4.0 L flasks at room temperature with orbital shaking at 250 rpm. For protein purification, cultures were centrifuged, and cell pellets were resuspended in 15 mL of CS binding buffer (50 mM Tris; 500 mM NaCl; 25 mM imidazole; pH 8.0). Cells were lysed by two passes through a French® pressure cell operated at 16,000 psi. The lysate was centrifuged (60,000×*g*, 30 min), and the supernatant was purified with a Ni-chelate HisTrap HP column (GE Healthcare Life Sciences). The elution buffer contained 50 mM Tris, 500 mM NaCl, 500 mM imidazole and 5 mM 2-mercaptoethanol (BME; pH 8.0). The purified proteins were dialyzed extensively into enzyme assay buffer (200 mM Tris pH 8.1) before assessing their catalytic activity. Protein concentrations were estimated from 280 nm absorbance in a Nanodrop spectrophotometer (Thermo-Fisher Scientific, Waltham, MA, USA) using an extinction coefficient of

40,340 $M^{-1}cm^{-1}$ calculated by the ExPASy ProtParam tool.

2.6. Enzyme assay

Citrate synthase catalyzes the reaction between acetyl-CoA and oxaloacetate to form citrate and CoA with a free thiol group (CoA-SH). Measurement of activity in 200 mM Tris buffer was based on the reaction between 5,5′-Dithiobis (2-nitrobenzoic acid) (DTNB) and CoA-SH which forms TNB detected at a wavelength of 412 nm (Srere et al., 1963). One unit of activity is the amount of enzyme that generates 1 μmol of CoA in 1 min at 37 °C. For the measurement of k_{cat} and apparent $K_{M(acetyl\text{-}CoA)}$, the oxaloacetate concentration of 10 mM was fixed, 5–7 different concentrations of acetyl-CoA were used (100 μM–4000 μM), and the results were fit to a nonlinear regression Michaelis-Menten enzyme kinetic model using JMP (SAS, Cary, NC, USA).

3. Results

3.1. Strain construction

The objective of this study was to reduce the catalytic activity of citrate synthase and thereby direct more acetyl-CoA to acetate as a model product derived from acetyl-CoA (Fig. 1). We hypothesized that reducing the intrinsic activity of citrate synthase, thus constricting the flux through that conduit, would increase the availability of acetyl-CoA and ultimately formation of acetate as a model product generated by *E. coli* from acetyl-CoA. In order to test this hypothesis, different point mutations in citrate synthase were introduced into the chromosome of *E. coli* Δ*poxB*.

Of course, several residues have previously been demonstrated to be critical to the functioning of citrate synthase. In an effort to prevent inactivation of the enzyme, for example, we did not target residues comprising the acetyl-CoA active site: H229, H264, H305, R314, D362, R387, and R407 (Pereira et al., 1994). Instead, using the 3-dimensional structure of citrate synthase for visual reference, we proposed residues that might affect the conformational space of the active site and decrease the affinity for acetyl-CoA binding. For example, three residues selected (W260, V361, and M372) appear to interact with residues H264 and D362 involved in acetyl-CoA binding. Likewise, residues 267–297 form the mobile loop, which situates acetyl-CoA in the active site (Duckworth et al., 2013). Given that acetyl-CoA binding promotes substantial structural shifts before the enzyme catalyzes the reaction, other residues were selected based on their spatial location near acetyl-CoA within the mobile loop (A267, G286 and S297). Mutations in residue S376 were expected to have a minimal effect on the activity since this residue is relatively close to the mobile loop but not the active site. In addition, we included F383 since previous studies noted this residue is conserved in citrate synthases and is proposed to stabilize the transition state (Pereira et al., 1994). To the best of our knowledge, the other residues assessed have not been previously studied. The criteria to choose specific point mutations were the hydrophobicity, polarity and charge of the residue to affect van der Waals and electrostatic forces, and/or modify the conformation of the active site residues in GltA.

Based on our inspection of the atomic structure of citrate synthase (Duckworth et al., 2013), eight different residues close to the active site and mobile loop were to be a target locus to mutate for the construction of *gltA* variants. From 31 plasmids constructed having point mutations in citrate synthase (Supplementary Materials Table S1), 29 strains of *E. coli* were successfully constructed containing the reintroduced wild-type *gltA* (1 strain), single point mutations (24 strains) or two point mutations (4 strains, Table 1). To examine the effect of these citrate synthase variants on growth and acetate formation, we used *E. coli* strains with a Δ*poxB* background. Therefore, acetate generated was derived primarily from acetyl-CoA via phosphotransacetylase-acetate kinase and not from pyruvate via pyruvate oxidase (Fig. 1).

3.2. Comparison of gltA variants in shake flasks

To compare the performance of the strains containing a citrate synthase variant, we first examined the growth rate and acetate generation of the 29 gltA variants in shake flask experiments using 5 g/L glucose as the sole carbon source. Of the wild-type and 24 single-point-mutation variants examined, 22 strains grew on glucose (Fig. 2). No growth was observed after 30 h for the variants having A267L, A267V or W260P mutations in citrate synthase. The strain with the native *gltA* (MEC882) attained a specific growth rate of 1.01 ± 0.02 h^{-1}, and no variant achieved a greater specific growth rate. Modification of W260 consistently resulted in a strain with a growth rate significantly lower than MEC882. For instance, W260V showed a growth rate of 0.33 ± 0.01 h^{-1} while W260F attained a growth rate of 0.72 ± 0.01 h^{-1}. Several of the specific mutations of V361, and the A267T variant also attained growth rates more than 25% lower than MEC882. In contrast, several single point mutations resulted in less than a 5% decrease in specific growth rate compared to the wild-type citrate synthase (E286D, S297M, S297T, V361I, M372S, S376H).

The wild-type and 24 single-point-mutation variants displayed a range of acetate formation from 5 g/L glucose in shake flasks (Fig. 2). The strain with wild-type citrate synthase (MEC882) showed an acetate yield of 0.05 ± 0.01 g/g glucose. Modification of residues W260, A267, and V361 generally increased acetate yield the greatest, while modification of residues F383, M372 and S297 also increased acetate yield compared to the wild-type variant, but to a lower extent (Fig. 2). More than 80% of the variants resulted in an acetate yield significantly greater than the wild-type strain, with strains carrying specific single-point-mutations of W260H, W260V, A267T, V361A, V361Q and V361T attaining acetate yields greater than 0.20 g/g glucose, four-fold greater than the wild-type citrate synthase. In contrast, strains harboring E286D, S376H and S376T mutations in citrate synthase generated less acetate than the strain with wild-type citrate synthase.

In addition to the 25 single-point-mutation/wild-type variants, we also constructed 4 variants having double-residue mutations, and 3 of these strains grew on glucose (Fig. 2). These three double-point-mutation variants were selected based on results from three single-point-mutation variants and represented a range of effects observed from the single-point-mutation variants: [W260F; V361A] (two mutations which resulted, individually, in relatively high acetate yield), [V361A; M372S] (one mutation showing high acetate yield, and a second with smaller acetate yield relative to the wild-type) and [S297M; M372S] (two mutations which resulted in small changes in acetate yield). Interestingly, the [W260F; V361A] variant resulted in the lowest specific growth rate (0.276 h^{-1}) and the greatest acetate yield (0.251 g/g) of all variants examined which grew on glucose as the sole carbon source. In contrast, the [S297M; M372S] variant showed no statistical difference in acetate yield compared to either of the single-point-mutation variants (i.e., S297M or M372S). In summary, the residues which resulted in a statistically lower growth rate and greater acetate yield compared to the wild-type citrate synthase were: W260F, W260H, W260I, W260T, W260V, A267T, V361A, V361T, M372K, F383M, [V361A; M372S] and [V361A; W260F].

No typical fermentation mixed-acid by-products (ethanol, lactate, succinate, formate) were detected during the culture of any of the variants. However, several of the variants accumulated pyruvate: V361A (pyruvate yield of 0.01 g/g), V361Q (0.05 g/g), A267T (0.03 g/g), W260V (0.02 g/g) and [V361A; W260F] (0.03 g/g).

We noted that a strain having a high acetate yield seemed to correspond with that strain having a lower growth rate, suggesting a negative correlation between these two variables. Indeed, a comparison of these two measured variables indicates a correlation ($R^2 = 0.782$, Fig. 3): the lower the growth rate, the higher acetate yield. All variants studied that showed a growth rate greater than 0.75 h^{-1} resulted in an acetate yield less than 0.10 g/g; all variants having a growth rate less than 0.75 h^{-1} attained an acetate yield greater than 0.10 g/g. Despite this correlation,

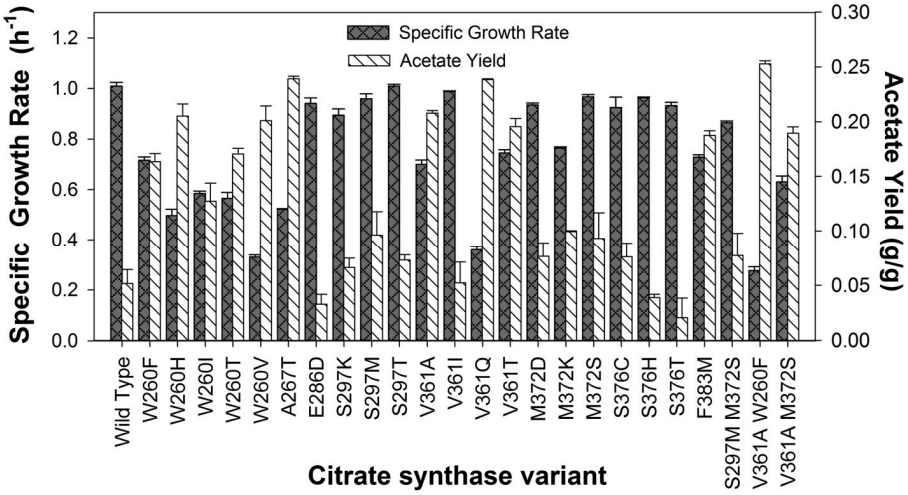

Fig. 2. Specific growth rate (dark bars) and acetate yield (light bars) of *E. coli* C Δ*poxB* variants containing different mutations in citrate synthase (*gltA* gene). The "Wild Type" variant is *E. coli* C Δ*poxB* with the native *gltA* gene (MEC882). All results represent triplicate shake flask experiments (error bars are standard deviations).

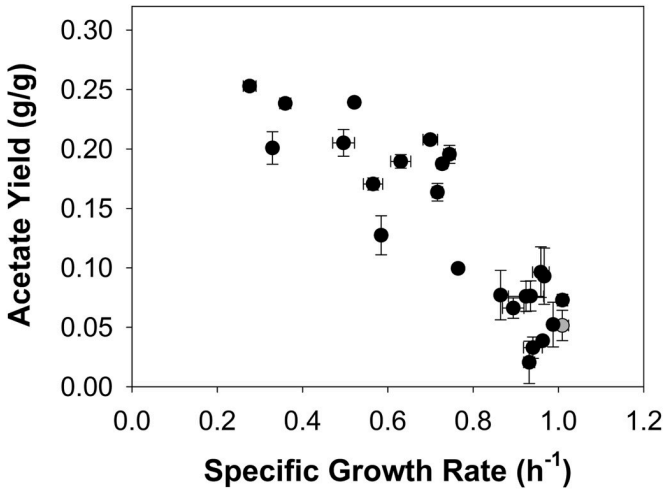

Fig. 3. Correlation between observed specific growth rate and observed acetate yield of *E. coli* Δ*poxB* variants containing different mutations in citrate synthase (*gltA* gene). The wild-type variant (shown as gray circle) is *E. coli* C Δ*poxB* with the native *gltA* gene (MEC882). All results represent triplicate shake flask experiments (error bars are standard deviations).

some strains deviated markedly from the average trend. For example, the strains having W260V or V361T mutations both achieved an acetate yield of about 0.20 g/g, but the W260V variant showed a growth rate of 0.33 ± 0.01 h^{-1} while V361T variant attained more than twice the specific growth rate (0.75 ± 0.01 h^{-1}).

3.2.1. Batch processes

Based on results from screening strains in shake flask experiments, we next examined specific variants in duplicate at the 1.0 L scale in controlled bioreactors using defined medium containing 15 g/L glucose. We selected four strains having the Δ*poxB* background for these aerobic batch processes: the strain with the native citrate synthase (MEC882), and variants V361A (MEC884), A267T (MEC890) and V361Q (MEC937). These variants not only attained high acetate yield in shake flasks, but also showed a statistically significant lower growth rate compared to the wild-type. Example batch results are shown in Fig. 4, and key parameters of these experiments are shown in Table 2. Similar to results from the shake flask studies, by-products including formate, succinate, lactate, ethanol, and also pyruvate were not detected (<0.02 g/L). MEC882 (wild-type *gltA*) reached an OD of 16 in about 6 h and generated acetate late in the process when glucose was almost depleted, accumulating 0.71 g/L acetate at the end of the process, corresponding to a yield of 0.049 g/g. In contrast, the other three strains examined which each contained a single *gltA* point mutation, reached an OD less than 14 in 8–16 h and generated about 4-fold more acetate than MEC882 (Table 2). These *gltA* variants began to accumulate acetate at the onset of the fermentation, much earlier than MEC882 containing the wild-type citrate synthase (Fig. 4). The greatest accumulation of acetate was observed with MEC890 containing the A267T mutation. Although these bioreactor studies provide relatively controlled environmental conditions compared to the previous shake flask studies (*e.g.*, oxygenation and pH change), the observed specific growth rates and acetate yields between the two sets of experiments were consistent. Because MEC890 (A267T variant) had the highest yield of acetate in the batch processes of those three variants studied, MEC890 and the wild-type strain (MEC882) were selected for chemostat experiments using glucose as the sole carbon source.

3.2.2. Steady-state processes

Chemostat systems complement the study of cell metabolism since they avoid time-dependent changes in specific growth rates and in availability of extracellular substrates which can limit the analysis of cause and effect (Folson and Carlson, 2015). Chemostat processes limit one or multiple nutrients, with carbon (C) and nitrogen (N) limitation as the most frequently studied (Hua et al., 2004). N-limitation is commonly used in bioprocesses to induce accumulation of carbon products such as polyhydroxyalkanoates (PHAs) (Keshavarz and Roy, 2010), while C-limitation is important to study acetate overflow metabolism in *E. coli* (Vemuri et al., 2006). The typical variables used to compare directly when analyzing acetate overflow are specific acetate formation rate (q_{Ace}, mmol/gh) as a function of specific glucose consumption rate (q_{Glu}, mmol/gh) (Eiteman and Altman, 2006). In order to assess further the effect of the *gltA* variants on the metabolism of *E. coli* and the production of acetate, we performed independent chemostat experiments under C-limited or N-limited conditions, achieved by limiting either glucose or ammonium.

Under N-limited conditions at a growth rate of 0.2 h^{-1}, the acetate yield on glucose ($Y_{Ace/Glu}$) averaged 0.12 g/g for MEC882, while $Y_{Ace/Glu}$ was 50% greater for MEC890 at 0.18 g/g. The specific glucose uptake rate was 5.6 mmol/gh for MEC882, while the specific rate of acetate formation was 2.1 mmol/gh. In contrast, for MEC890 the specific glucose uptake rate was 5.3 mmol/gh, while the specific rate of acetate formation was 2.9 mmol/gh. Thus, the specific acetate formation rate

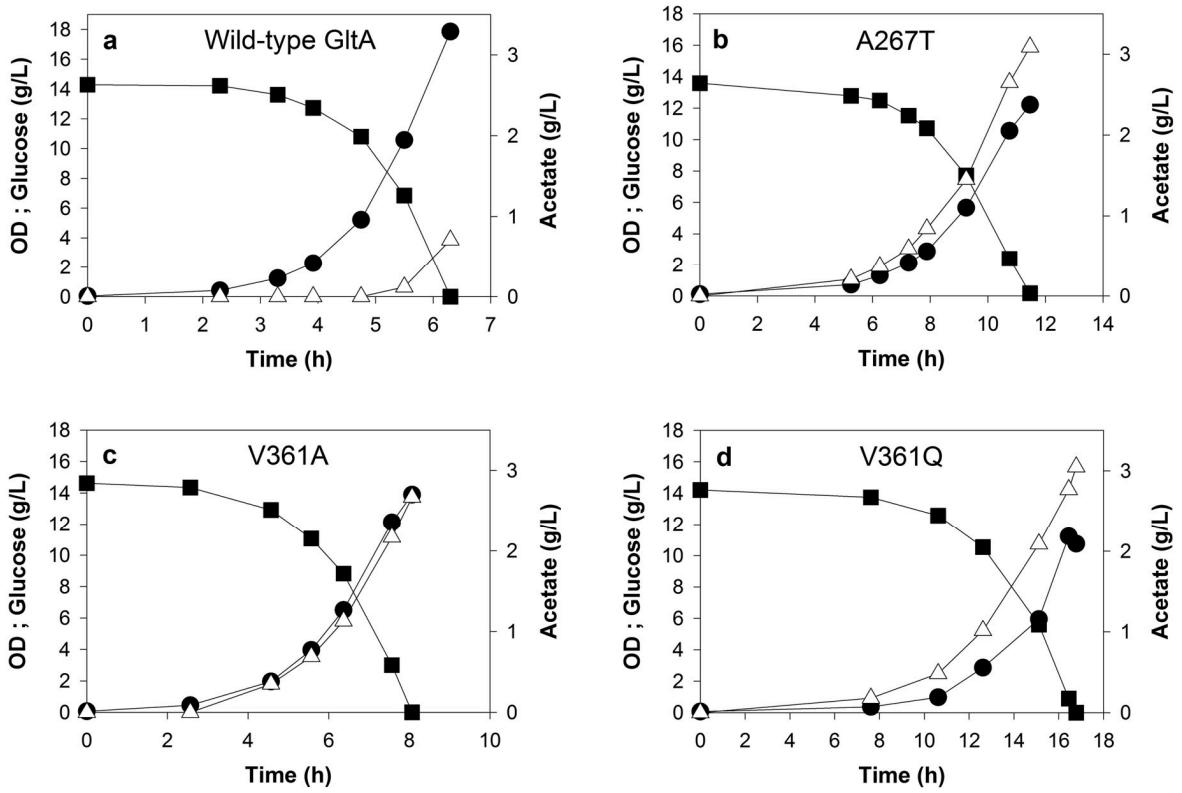

Fig. 4. Acetate generation from glucose during 1.0 L batch fermentations of selected citrate synthase variants: OD (●), glucose (■), acetate (△). Strains compared were (a) MEC882 (wild-type citrate synthase), (b) MEC890 (A267T variant), (c) MEC884 (V361A variant), (d) MEC937 (V361Q variant).

Table 2
Biomass yield, acetate yield and specific growth rate during 1.0 L controlled batch process using *E. coli* C Δ*poxB* with single point mutations in the citrate synthase enzyme. Mean and standard deviation are shown.

Citrate Synthase variant	Biomass yield (g/g)	Acetate yield (g/g)	Specific Growth Rate (h^{-1})
native GltA	0.411 ± 0.018	0.049 ± 0.001	0.939 ± 0.039
GltA[A267T]	0.317 ± 0.001	0.237 ± 0.005	0.415 ± 0.009
GltA[V361A]	0.339 ± 0.006	0.187 ± 0.003	0.684 ± 0.027
GltA[V361Q]	0.301 ± 0.018	0.182 ± 0.023	0.370 ± 0.012

was greater in the A267T variant at a dilution rate of 0.2 h^{-1} despite the lower glucose uptake rate. Acetate generation rate was much greater with the strain containing the A267T mutation in *gltA* than with the wild-type, as expected.

Under C-limited conditions, specific growth rates (i.e., dilution rates) of 0.14 h^{-1} – 0.30 h^{-1} were examined in independent chemostat experiments for MEC882 and MEC890 (Fig. 5). In this range of growth rates, MEC882 harboring the wild-type citrate synthase surprisingly did not form acetate. In contrast, MEC890 containing the A267T mutation generated significant acetate at the nominal dilution rates of 0.20 h^{-1} and 0.30 h^{-1}. At 0.20 h^{-1}, the acetate yield on glucose ($Y_{Ace/Glu}$) averaged 0.14 g/g, with a specific glucose uptake rate of about 2.7 mmol/gh and an acetate formation rate of 1.1 mmol/gh. At 0.30 h^{-1}, $Y_{Ace/Glu}$ was 0.11 g/g, with a specific glucose uptake rate of 3.9 mmol/gh, and an acetate formation rate of 1.3 mmol/gh (Fig. 5). The A267T variant responded quite differently at steady-state than MEC882 harboring the wild-type citrate synthase: no acetate was observed from C Δ*poxB* (with the native *gltA*), at least when the glucose uptake rate was less than 4.0 mmol/gh. Acetate was formed in C Δ*poxB gltA*[A267T] when the glucose uptake rate reached about 2.7 mmol/gh.

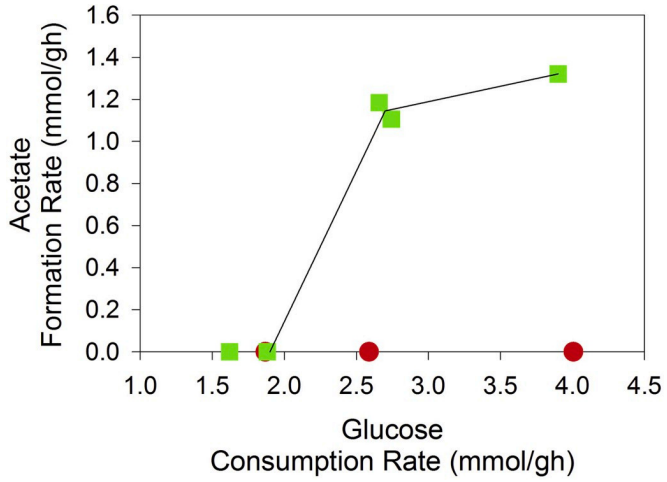

Fig. 5. Steady-state formation of acetate from glucose as the sole carbon source. MEC882 (C Δ*poxB*, ●) and MEC890 (C Δ*poxB gltA*[A267T], ■) were grown in chemostats under carbon-limited conditions at dilution rates of 0.14 h^{-1} – 0.30 h^{-1}.

3.2.3. Catalytic activity of citrate synthase

Since MEC890 harboring the A267T mutation in citrate synthase showed greater acetate formation in *E. coli* C Δ*poxB* than the strain with the wild-type enzyme, we next measured the kinetic parameters (K_M and k_{cat}) of the two purified enzymes. The k_{cat} and apparent $K_{M(acetyl\text{-}CoA)}$ were measured using initial reaction rate data in the presence of 6–7 different acetyl-CoA concentrations and fitting these values with a non-linear regression model using the Michaelis-Menten equation. In these measurements, a constant oxaloacetate concentration (10 mM) was maintained, and therefore we report "apparent" kinetic parameters.

Although the A267T and other mutations may have altered oxaloacetate binding and the formation of the transition state, given the low value for the K_M (oxaloacetate) for GltA at 26 μM (Pereira et al., 1994), the $K_{M\ (acetyl\text{-}CoA)}$ for GltA[A267T] reported here could be considered a "true" Michalis constant.

The A267T substitution indeed did significantly alter the kinetic parameters of the enzyme (Table 3). Specifically, the citrate synthase with the A267T mutation showed a two-fold increase in apparent K_M compared to the wild-type, and a turnover number (k_{cat}) approximately sixteen times lower than the wild-type citrate synthase. These results demonstrate a decrease in the specificity constant (k_{cat}/K_M) of citrate synthase resulting from the A267T mutation.

Although the k_{cat}/K_M ratio can be a useful index for comparing the relative rates of one enzyme acting on alternative or competing substrates, it is not as useful when comparing the catalytic effectiveness of two enzymes acting on the same substrate (Eisenthal et al., 2007). As noted by Ceccarelli et al., (2008), k_{cat}/K_M estimates enzyme efficiency only for the unrealistic case of a zero substrate concentration. As a preferred parameter, the efficiency function (E_f) is essentially a dimensionless first-order rate constant and offers a better comparison of different enzymes catalyzing the same reaction (Carrillo et al., 2010). Importantly, E_f includes the effects of substrate concentration and diffusion (Ceccarelli et al., 2008). Therefore, we also determined E_f to compare the wild-type GltA and the GltA[A267T] variant (Fig. 6). The calculated efficiency function for both enzymes decreases as the substrate acetyl-CoA concentration increases (because the reaction becomes zeroth order), but the A267T variant has a 16–38 × lower efficiency than the native citrate synthase at all concentrations of acetyl-CoA.

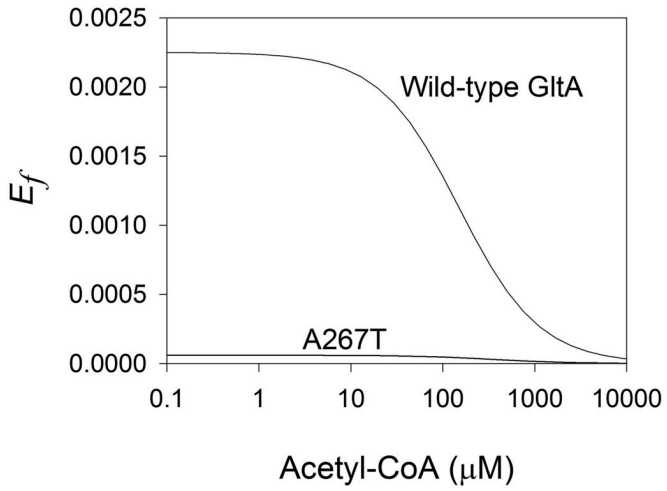

Fig. 6. Efficiency function (E_f) for wild-type citrate synthase and the GltA [A267T] variant as a function of acetyl-CoA concentration in the absence of product inhibition.

4. Discussion

4.1. Citrate synthase plays a significant role in the flux of acetyl-CoA

Acetyl-CoA is a key central metabolite and precursor for the microbial production of many industrially relevant biochemicals (Krivoruchko et al., 2015). Moreover, studies with *E. coli* at steady-state, aerobic conditions have shown that the largest metabolic drain of acetyl-CoA is to the TCA cycle via the enzyme citrate synthase (Zhao et al., 2004). Unfortunately, merely knocking out citrate synthase prevents *E. coli* growth on glucose as a sole carbon source (Wu and Eiteman, 2016). Instead of eliminating citrate synthase, we aimed to decrease the intrinsic catalytic activity of the enzyme through genetic modification of residues thought to affect the conformational structure around the acetyl-CoA binding pocket (i.e., affect k_{cat} and/or K_M). Therefore, 28 new *E. coli* C strains containing single- or double-point mutations in citrate synthase were examined, along with a wild-type citrate synthase, for their growth and acetate production. All strains possessed a Δ*poxB* knockout to prevent the decarboxylation of pyruvate to form acetyl-CoA, and thus acetate formation could be attributed primarily to the hydrolysis of acetyl-CoA via phosphotransacetylase-acetate kinase pathway (Fig. 1).

4.2. Point mutations in citrate synthase modify the enzyme

In our study, point mutations at A267 and V361 significantly impacted growth rate and acetate yield, despite the indirect interaction between these residues and the acetyl-CoA active site (Pereira et al., 1994). This result is consistent with the observation that the most abundant amino acid pairs found in proteins involve Leu, Val, Ile and Ala, where interactions with these amino acids can confer protein properties (Petersen et al., 2012). Indeed, only one variant (A267T) of the three A267 mutations constructed was even able to grow, suggesting that this residue is critical to the mobile loop flexibility. Though only three variants at A267 were examined, the substitution of a larger hydrophobic amino acid (leucine or valine) appears to be more detrimental to citrate synthase activity than a change to a polar amino acid (threonine). Additional crystallography studies could provide conformational evidence of how A267 mutations affect acetyl-CoA binding.

Table 3
Measured kinetic parameters of His_6-tagged wild-type GltA and GltA[A267T]. Mean and standard deviation are shown.

Citrate Synthase Variant	$K_{M(acetyl\text{-}CoA)}$ (μM)	k_{cat} (s^{-1})
Wild-type GltA	151 ± 34	34 ± 3.0
GltA[A267T]	351 ± 93	2.1 ± 0.2

4.3. Point mutations in citrate synthase affected growth rate

None of the GltA variants constructed showed a significantly higher growth rate in shake flasks than the strain containing the wild-type GltA. Since the specific mutations were selected to reduce catalytic activity, the lack of a faster growing strain is unsurprising, and does not demonstrate wild-type GltA is the growth-optimal enzyme. All significantly slower growing strains generated acetate: indeed, acetate formation correlated with growth rate (Fig. 3). These results suggest that constriction of flux at citrate synthase generally leads to increased acetate and slower growth, and that acetate formation serves as a natural "relief valve" when flux into the TCA cycle is slowed. Acetate overflow in *E. coli* is also attributed to saturation of respiration (Vemuri et al., 2006). However, citrate synthase mutations examined herein targeted acetyl-CoA binding, and we did not specifically aim to affect acetate formation through the allosteric binding of NADH with citrate synthase. Thus, we would not expect any of the constructed variants to affect *E. coli* metabolism under anaerobic conditions.

The decreased growth rate observed with citrate synthase variants could be attributed to several causes. An increased pool of acetyl-CoA would likely have multiple and complex effects. Elevated acetyl-CoA inhibits cell growth (Morgan and Kornberg, 1969) and the E2 component of the pyruvate dehydrogenase complex (PDHc) (Kok et al., 1998), potentially slowing glycolysis. Several variants did indeed accumulate some pyruvate under shake flask conditions, demonstrating how a constriction at the acetyl-CoA node may propagate upstream of citrate synthase. Any pyruvate accumulation resulting from an increased pool of acetyl-CoA would promote the phosphorylation of ArcA, a global protein regulator that controls the expression of numerous genes associated in energy metabolism (Förster and Gescher, 2014). The accumulation of pyruvate or acetyl-CoA also slows glucose uptake in response to high levels of these precursors (Yang et al., 2001).

Diminished citrate synthase activity would likely slow the TCA cycle. The TCA cycle not only completes the oxidation of acetyl-CoA to produce CO_2, ATP and reducing equivalents, it also serves to generate several amino acids as biosynthetic precursors (Shiloach and Rinas, 2009; Kwong et al., 2017). Thus, restricting flux through the TCA cycle could in extreme cases limit ATP formation and productivity. Fortunately, *E. coli* increases glucose uptake in response to reduced ATP generation (Koebmann et al., 2002; Zhu et al., 2008). A reduced citrate synthase activity would also tend to increase the oxaloacetate pool, which might reduce the anaplerotic flux (PEP carboxylase, PEP carboxykinase) necessary to support the formation of TCA cycle precursors.

Mere exposure of *E. coli* cells to high acetate concentrations is known to decrease growth rate. Various studies have reported 2.4–6 g/L acetate retards *E. coli* growth rate (Luli and Strohl, 1990; Lasko et al., 2000; Dittrich et al., 2005a). Explanations for acetate growth inhibition include alteration of the membrane potential, inhibition of enzyme activity, and interference with the regulatory functions of acetate-phosphate (Wolfe, 2005; Pinhal et al., 2019). Our controlled batch experiments showed a 2-fold reduction in growth rate for the variants V361A, V361Q and A267T, which each generated >2.5 g/L acetate. However, growth rates during these experiments were measured before acetate had accumulated to that concentration, and therefore the mere presence of acetate seems unlikely to be the direct cause of suppressed growth. More likely, the rate of acetate formation itself, and the diversion of carbon to this end product, affects growth rate.

4.4. Acetate metabolism by engineered strains

Acetate is mainly produced from acetyl-CoA via acetyl phosphate by phosphotransacetylase (*pta* gene) and acetate kinase (*ackA*) or from pyruvate by pyruvate oxidase (*poxB*) (Fig. 1). Acetate consumption produces acetyl-CoA through acetyl-AMP by acetyl-CoA synthetase (*acs*), and by the reverse reaction of phosphotransacetylase-acetate kinase (Shiloach and Rinas, 2009). Our studies do not establish the extent to which the acetate generated by these variants is re-assimilated by either of these pathways.

Biotechnological production of acetate is based on the oxidation of ethanol by *Acetobacter* and *Komagataeibacter* strains that have high acetic acid and ethanol tolerance (Saichana et al., 2015). An advantage of engineering *E. coli* strains for acetate production is the possibility of using carbon sources other than ethanol (Förster and Gescher, 2014). An acetate yield from glucose of 0.58 g/g was reported in a genetically modified strain of *E. coli* by combining in fermentative and respiratory strategies to establish a homoacetate pathway (Causey et al., 2003). Recently, a synthetic non-oxidative glycolysis pathway was introduced in *E. coli* which can theoretically produce 1.00 g/g acetate from glucose (Bogorad et al., 2013; Lin et al., 2018).

In the present study, we attained acetate yields of 37% of the theoretical yield under fully aerobic conditions only by deleting *poxB* and modifying GltA. One would anticipate a greater yield in strains having the additional *acs* knockout. Importantly, with this strategy we obtained a range of acetate accumulation (Fig. 2); the variants examined offer a spectrum of citrate synthase activities and acetate yields. Strains from this collection could thus be screened, after additional knockouts were introduced (*e.g.*, *pta*, *ackA*, *acs*), for the formation of any acetyl-CoA-derived product based on the desired balance between growth rate and product formation. Given the effect of citrate synthase on ATP generation and biosynthesis, an appropriate citrate synthase variant should be selected to match the specific design requirements.

4.5. Metabolism of E. coli at steady-state

Steady-state experiments of *E. coli* C Δ*poxB* under N-limited conditions allow carbon flux to occur at its regulatory capacity. The specific glucose uptake rate obtained (q_{glu}, 5.6 mmol/gh) for the wild-type GltA strain MEC882 was similar to those reported for *E. coli* BW25113 (4.7 mmol/gh) and *E. coli* K-12 MG1655 (6.2 mmol/gh) under similar steady-state N-limited conditions (Kumar and Shimizu, 2011; Folson and Carlson, 2015). The specific glucose uptake rate was slightly decreased for the A267T variant strain MEC890 (5.3 mmol/gh). The yield of acetate observed for MEC882 (0.120 g/g) is 30–50% lower than other steady-state N-limited studies using other *E. coli* strains at 0.2 h^{-1}, which had acetate yields of 0.20 g/g (for *E. coli* BW25113), 0.25 g/g (K-12 MG1655) and 0.18 g/g (K-12 W3110) (Kumar and Shimizu, 2011; Folson and Carlson, 2015; Hua et al., 2004).

In this study, the GltA[A267T] variant showed greater acetate yield than the wild-type GltA in both batch and N-limited steady-state processes. Typically, N-limited (and therefore C-excess) conditions allow for the greater yield of microbial products such as polyhydroxyalkanoates (Keshavarz and Roy, 2010), biofuels (Sharma et al., 2012) and fatty acids (Marella et al., 2017). As expected, N-limited conditions increased acetate yield of the wild-type strain (MEC882) compared to batch conditions (0.12 g/g versus 0.05 g/g). However, the acetate yield for A267T variant (MEC890) was lower under steady-state N-limited conditions compared to batch conditions. Why did MEC890 show an acetate yield of 0.21 g/g under batch conditions (growth rate of 0.42 h^{-1}) but a yield of 0.18 g/g under steady-state N-limited conditions (at a growth rate of 0.20 h^{-1})? Obviously, carbon metabolism, nitrogen assimilation, and energy generation are integrated and respond to nutrient limitation (Kumar and Shimizu, 2011). Many transporters are transcriptionally regulated, and as the availability of specific nutrients declines, classes of higher affinity transporters are expressed (Gresham and Hong, 2015). Also, the *acs* gene coding acetyl-CoA synthase was not deleted, and thus any strain could use this route and Pta-AckA to metabolize acetate. Such acetate utilization would likely differ between nutrient-excess batch and nutrient-limited continuous growth conditions. Proteomic or transcriptional analysis of central metabolism enzymes could provide more clarification.

4.6. Variants of citrate synthase altered the catalytic activity of the enzyme

Changes in selected residues of GltA impacted its catalytic activity and profoundly altered the metabolism of *E. coli* to redirect carbon to acetate. The observations that the apparent $K_{M(acetyl\text{-}CoA)}$ for GltA[A267T] was twice as great as the native GltA, the k_{cat} sixteen times lower, and the efficiency function 16–38 times lower, provide evidence that the flux through citrate synthase was reduced. Other studies on citrate synthase have also examined mutations in specific residues of the enzyme, but for different purposes. For example, in an effort to introduce more stability into the mobile loop region and to facilitate crystallographic studies with bound substrates, an amino acid sequence of five residues from *Acetobacter aceti* was substituted into *E. coli* resulting in kinetic parameters of k_{cat} of 21 s^{-1} and $K_{M(acetyl\text{-}CoA)}$ of 225 μM (Duckworth et al., 2013). In another study, citrate synthase mutations were discovered during the Lenski long-term evolution experiment (LTEE) affecting the NADH binding pocket, resulting in $K_{M(acetyl\text{-}CoA)}$ values 2.7-fold and 2.1-fold greater than the native *gltA* respectively for variants GltA[A258T; A162V] and GltA[A258T; A124T]. For these variants the k_{cat} values were close to or greater than the wild-type enzyme (Quandt et al., 2015). However, mutations in *gltA* were rare in this evolution process. Only one mutation in citrate synthase was found among 16 clones isolated at generations 20,000 to 40,000 from 7 LTEE populations (Wielgoss et al., 2011).

The kinetic parameters obtained for GltA[A267T] support the strategy of targeted mutations of citrate synthase to increase the production of biochemicals derived from acetyl-CoA. An elevated $K_{M(acetyl\text{-}CoA)}$ for citrate synthase (*e.g.*, from 151 μM to 351 μM) would decrease affinity of the enzyme towards acetyl-CoA, making this enzyme less competitive with an enzyme leading to a desired product derived from acetyl-CoA. For example, citrate synthase is competing with

phosphotransacetylase which possesses a turnover number (k_{cat}) of 29.6 s^{-1}, and has sigmoidal kinetics with a Hill coefficient of 1.3 (effective $K_{M\ (acetyl\text{-}CoA)}$ of 141 μM) (Campos-Bermudez et al., 2010). *E. coli* cultures have reported concentrations in the range of 20–600 μM during aerobic batch growth on glucose (Vallari et al., 1987; Takamura and Nomura, 1988). In this range of intracellular acetyl-CoA in the absence of effectors, assuming that the enzyme concentration has not changed, the GltA [A267T] variant would have a flux of 20–37 times smaller than GltA (at the same acetyl-CoA concentration). At 20 μM acetyl-CoA, native citrate synthase would attain a rate relative to its maximum turnover of 12% (4.0 s^{-1}), the A267T variant would attain a relative rate of 7.4% (0.15 s^{-1}), while phosphotransacetylase would attain a rate of 7.6 s^{-1}. At 600 μM acetyl-CoA, native citrate synthase would attain a rate of 80% of its maximum turnover (27 s^{-1}), the A267T variant would attain a rate of 1.3 s^{-1}, while phosphotransacetylase would attain a rate of 29 s^{-1}. Thus, at 20 μM acetyl-CoA, phosphotransacetylase has nearly twice the intrinsic activity (per enzyme molecule basis) toward acetyl-CoA than the wild-type citrate synthase, but 51-fold greater activity than GltA [A267T]. At 600 μM acetyl-CoA, phosphotransacetylase has nearly the same activity toward acetyl-CoA than citrate synthase, but 22-fold greater activity than GltA[A267T]. This analysis demonstrates that reducing the activity of central metabolic enzymes at key metabolic branchpoints through the modification of kinetic parameters can be a very effective approach to making a pathway more competitive with central metabolic pathways and increase the flux toward pathways toward biochemicals of interest.

4.7. A reduced flux in citrate synthase can favor the production of biochemicals derived from acetyl-CoA

Altering the activity of citrate synthase complements other approaches which involve modulation of citrate synthase expression. For example, altering the promoter of *gltA* led to 10%–100% of the native expression, with the optimal modulation resulting in an increase in lysine yield from 0.17 mol/mol to 0.31 mol/mol (van Ooyen et al., 2012). Similarly, a toggle switch can be designed at key nodes such as citrate synthase, an approach which uses a conditional knockout that effectively shuts off flux (Soma et al., 2014). Whereas modifying promoter strength alters the quantity of a target enzyme expressed, modifying the residues on a target enzyme could affect substrate and effector affinities, turnover, and potentially the nature of the reaction (allosteric regulation). Also, the targeted, chromosomal modification of an enzyme does not create the need for additional triggers and likely does not alter the metabolic burden of the enzyme, in contrast to strategies which rely on inducer molecules (Wang et al., 2018). Reducing the activity of a competing enzyme, in contrast to outright elimination of expression, would allow the use of a chemostat mode of production. Ultimately, these strategies all share the goal of balancing the pool of acetyl-CoA with growth to facilitate the formation of a product of interest. The strategy of reducing the activity of a competing enzyme like citrate synthase can be used alone or complement these other strategies to improve the production of biochemicals derived from acetyl-CoA.

CRediT authorship contribution statement

D. Brisbane Tovilla-Coutiño: Methodology, Validation, Formal analysis, Investigation, Writing - original draft. **Cory Momany:** Methodology, Supervision, Writing - review & editing. **Mark A. Eiteman:** Conceptualization, Formal analysis, Writing - review & editing, Supervision, Project administration, Funding acquisition.

Acknowledgments

The authors thank Sarah Lee, W. Chris Moxley and Ajay Arya for technical support in this research. The authors also thank the U.S. National Science Foundation (CBET-1802533) and Fulbright Degree Program administered by Laspau (Latin American Scholarship Program of American Universities) for financial support.

Appendix A. Supplementary data

Supplementary data to this article can be found online at https://doi.org/10.1016/j.ymben.2020.06.006.

References

Baba, T., Ara, T., Hasegawa, M., Takai, Y., Okumura, Y., Baba, M., Datsenko, K.A., Tomita, M., Wanner, B.L., Mori, H., 2006. Construction of *Escherichia coli* K-12 in-frame, single-gene knockout mutants: the Keio collection. Mol. Syst. Biol. 2 (1), 1–11.

Bogorad, I.W., Lin, T.S., Liao, J.C., 2013. Synthetic non-oxidative glycolysis enables complete carbon conservation. Nature 502, 693–697.

Campos-Bermudez, V.A., Bologna, F.P., Andreo, C., Drincovich, M.F., 2010. Functional dissection of *Escherichia coli* phosphotransacetylase structural domains and analysis of key compounds involved in activity regulation. FEBS J. 277, 1957–1966.

Carrillo, N., Ceccarelli, E.A., Roveri, O.A., 2010. Usefulness of kinetic enzyme parameters in biotechnological practice. Biotechnol. Genet. Eng. Rev. 27 (1), 367–382.

Causey, T.B., Zhou, S., Shanmugam, K.T., Ingram, L.O., 2003. Engineering the metabolism of *Escherichia coli* W3110 for the conversion of sugar to redox-neutral and oxidized products: homoacetate production. Proc. Natl. Acad. Sci. Unit. States Am. 100 (3), 825–832.

Ceccarelli, E.A., Carrillo, N., Roveri, O.A., 2008. Efficiency function for comparing catalytic competence. Trends Biotechnol. 26, 117–118.

Chen, V.C., Sadler, G., McComb, M.E., Perreault, H., Duckworth, H.W., 2011. Characterization of specific binding by mass spectrometry: associations of *E. coli* citrate synthase with NADH and 2-azidoATP. Int. J. Mass Spectrom. 305, 238–246.

Datsenko, K.A., Wanner, B.L., 2000. One-step inactivation of chromosomal genes in *Escherichia coli* K-12 using PCR products. Proc. Natl. Acad. Sci. Unit. States Am. 97, 6640–6645.

De Mey, M., De Maeseneire, S., Soetaert, W., Vandamme, E., 2007. Minimizing acetate formation in *E. coli* fermentations. J. Ind. Microbiol. Biotechnol. 34, 689–700.

Dittrich, C.R., Bennett, G.N., San, K.Y., 2005a. Characterization of the acetate-producing pathways in *Escherichia coli*. Biotechnol. Prog. 21, 1062–1067.

Dittrich, C.R., Vadali, R.V., Bennett, G.N., San, K.Y., 2005b. Redistribution of metabolic fluxes in the central aerobic metabolic pathway of *E. coli* mutant strains with deletion of the ackA pta and poxB pathways for the synthesis of isoamyl acetate. Biotechnol. Prog. 21, 627–631.

Donald, L.J., Crane, B.R., Anderson, D.H., Duckworth, H.W., 1991. The role of cysteine 206 in allosteric inhibition of *Escherichia coli* citrate synthase. J. Biol. Chem. 266 (31), 20709–20713.

Duckworth, H.W., Nguyen, N.T., Gao, Y., Donald, L.J., Maurus, R., Ayed, A., Bruneau, B., Brayer, G.D., 2013. Enzyme-substrate complexes of allosteric citrate synthase: evidence for a novel intermediate in substrate binding. Biochim. Biophys. Acta Protein Proteonomics 1834, 2546–2553.

Eisenthal, R., Danson, M.J., Hough, D.W., 2007. Catalytic efficiency and k_{cat}/K_M: a useful comparator? Trends Biotechnol. 25, 247–249.

Eiteman, M.A., Chastain, M.J., 1997. Optimization of the ion exchange analysis of organic acids from fermentation. Anal. Chim. Acta 338, 69–75.

Eiteman, M.A., Altman, E., 2006. Overcoming acetate in *Escherichia coli* recombinant protein fermentations. Trends Biotechnol. 24 (11), 530–536.

Enjalbert, B., Millard, P., Dinclaux, M., Portais, J.C., Létisse, F., 2017. Acetate fluxes in *Escherichia coli* are determined by the thermodynamic control of the Pta-AckA pathway. Sci. Rep. 7, 42135.

Folson, J.P., Carlson, R.P., 2015. Physiological, biomass elemental composition and proteomic analyses of *Escherichia coli* ammonium-limited chemostat growth, and comparison with iron- and glucose-limited chemostat growth. Microbiology 161 (8), 1659–1670.

Förster, A.H., Gescher, J., 2014. Metabolic engineering of *Escherichia coli* for production of mixed-acid fermentation end products. Frontiers in Bioengineering and Biotechnology 2 (16), 1–12.

Fuchs, G., Berg, I.A., 2014. Unfamiliar metabolic links in the central carbon metabolism. J. Biotechnol. 192 (Part B), 314–322.

Galloway, N., Toutkoushian, H., Nune, M., Bose, N., Momany, C., 2013. Rapid cloning for protein crystallography using type IIS restriction enzymes. Cryst. Growth Des. 13, 2833–2839.

Gresham, D., Hong, J., 2015. The functional basis of adaptive evolution in chemostats. FEMS (Fed. Eur. Microbiol. Soc.) Microbiol. Rev. 39, 2–16.

Hua, Q., Yang, C., Oshima, T., Mori, H., Shimizu, K., 2004. Analysis of gene expression in *Escherichia coli* in response to changes of growth-limiting nutrient in chemostat cultures. Appl. Environ. Microbiol. 70 (4), 2354–2365.

Keshavarz, T., Roy, I., 2010. Polyhydroxyalkanoates: bioplastics with a green agenda. Curr. Opin. Microbiol. 13, 321–326.

Kim, S., Seong, W., Han, G., Lee, D.-H., Lee, S.G., 2017. CRISPR interference-guided multiplex repression of endogenous competing pathway genes for redirecting metabolic flux in *Escherichia coli*. Microb. Cell Factories 16, 1–15.

Koebmann, B.J., Westerhoff, H.V., Snoep, J.L., Nilsson, D., Jensen, P.R., 2002. The glycolytic flux in *Escherichia coli* is controlled by the demand for ATP. J. Bacteriol. 184, 3909–3916.

Kok, A., Hengeveld, A.F., Martin, A., Westphal, A.H., 1998. The pyruvate dehydrogenase multi-enzyme complex from Gram-negative bacteria. Biochim. Biophys. Acta 1385, 353–366.
Krivoruchko, A., Zhang, Y., Siewers, V., Chen, Y., Nielsen, J., 2015. Microbial acetyl-CoA metabolism and metabolic engineering. Metab. Eng. 28, 28–42.
Kumar, R., Shimizu, K., 2011. Transcriptional regulation of main metabolic pathways of *cyoA, cydB, fnr*, and *Fur* gene knockout *Escherichia coli* in c-limited and n-limited aerobic continuous cultures. Microb. Cell Factories 10 (3), 1–15.
Kwong, W.K., Zheng, H., Moran, N.A., 2017. Convergent evolution of a modified, acetate-driven TCA cycle in bacteria. Nature Microbiology 2, 17067.
Lasko, D.R., Zamboni, N., Sauer, U., 2000. Bacterial response to acetate challenge: a comparison of tolerance among species. Appl. Microbiol. Biotechnol. 54 (2), 243–247.
Leonard, E., Lim, K.H., Saw, P.N., Koffas, M.A., 2007. Engineering central metabolic pathways for high-level flavonoid production in *Escherichia coli*. Appl. Environ. Microbiol. 73, 3877–3886.
Lin, F., Chen, Y., Levine, R., Lee, K., Yuan, Y., Lin, X.N., 2013. Improving fatty acid availability for bio-hydrocarbon production in *Escherichia coli* by metabolic engineering. PloS One 8, e78595.
Lin, P.P., Jaeger, A.J., Wu, T.Y., Xu, S.C., Lee, A.S., Gao, F., Chen, P.W., Liao, J.C., 2018. Construction and evolution of an *Escherichia coli* strain relying on nonoxidative glycolysis for sugar catabolism. Proceedings of the National Academy of Sciences USA 115 (14), 3538–3546.
Luli, G.W., Strohl, W.R., 1990. Comparison of growth, acetate production, and acetate inhibition of *Escherichia coli* strains in batch and fed-batch fermentations. Appl. Environ. Microbiol. 56, 1004–1011.
Marella, E.R., Holkenbrink, C., Siewers, V., Borodina, I., 2017. Engineering microbial fatty acid metabolism for biofuels and biochemicals. Curr. Opin. Biotechnol. 50, 39–46.
Matsumoto, K., Okei, T., Honma, I., Ooi, T., Aoki, H., Taguchi, S., 2013. Efficient (R)-3-hydroxybutyrate production using acetyl CoA-regenerating pathway catalyzed by coenzyme A transferase. Appl. Microbiol. Biotechnol. 97, 205–210.
Morgan, M.J., Kornberg, H.L., 1969. Regulation of sugar accumulation by *Escherichia coli*. FEBS (Fed. Eur. Biochem. Soc.) Lett. 3, 53–56.
Pereira, D.S., Donald, L.J., Hosfield, D.J., Duckworth, H.W., 1994. Active site mutants of *Escherichia coli* citrate synthase. J. Biol. Chem. 269, 412–417.
Petersen, S.B., Neves-Petersen, M.T., Henriksen, S.B., Mortensen, R.J., Geertz-Hansen, H. M., 2012. Scale-free behaviour of amino acid pair interactions in folded proteins. PloS One 7 (7), 1–14.
Pietrocola, F., Galluzzi, L., Bravo-San Pedro, J.M., Madeo, F., Kroemer, G., 2015. Acetyl coenzyme A: a central metabolite and second messenger. Cell Metabol. 21 (6), 805–821.
Pinhal, S., Ropers, D., Geiselmann, J., de Jong, H., 2019. Acetate metabolism and the inhibition of bacterial growth by acetate. J. Bacteriol. 201 e00147-19.
Pontrelli, S., Chiu, T.-Y., Lan, E.I., Chen, F., Chang, P., Liao, J.C., 2018. *Escherichia coli* as a host for metabolic engineering. Metab. Eng. 50, 6–46.
Quandt, E.M., Gollihar, J., Blount, Z.D., Ellington, A.D., Georgiou, G., Barrick, J.E., 2015. Fine-tuning citrate synthase flux potentiates and refines metabolic innovation in the Lenski evolution experiment. eLife 4, 1–22.
Saichana, N., Matsushita, K., Adachi, O., Frébort, I., Frebortova, J., 2015. Acetic acid bacteria: a group of bacteria with versatile biotechnological applications. Biotechnol. Adv. 33 (6), 1260–1271.
Saini, M., Li, S.-Y., Wang, Z.W., Chiang, C.-J., Chao, Y.-P., 2016. Systematic engineering of the central metabolism in *Escherichia coli* for effective production of n-butanol. Biotechnol. Biofuels 9, 1–10.
Sharma, K.K., Schuhmann, H., Schenk, P.M., 2012. High lipid induction in microalgae for biodiesel production. Energies 5 (5), 1532–1553.
Shiloach, J., Rinas, U., 2009. Systems biology and biotechnology of *Escherichia coli*. Nature 24, 377–400.
Soma, Y., Tsuruno, K., Wada, M., Yokota, A., Hanai, T., 2014. Metabolic flux redirection from a central metabolic pathway toward a synthestic pathway using a metabolic toggle switch. Metab. Eng. 23, 175–184.
Srere, P.A., Brazil, H., Gonen, L., 1963. The citrate condensing enzyme of pigeon breast muscle and moth flight muscle. Acta Chem. Scand. 17, S129–S134.
Studier, F., 2005. Protein production by auto-induction in high-density shaking cultures. Protein Expr. Purif. 41, 207–234.
Takamura, Y., Nomura, G., 1988. Changes in the intracellular concentration of acetyl-CoA and malonyl-CoA in relation to the carbon and energy metabolism of *Escherichia coli* K12. J. Gen. Microbiol. 134, 2249–2253.
Vallari, D.S., Jackowski, S., Rock, C.O., 1987. Regulation of pantothenate kinase by coenzyme A and its thioesters. J. Biol. Chem. 262, 2468–2471.
van Ooyen, J., Noack, S., Bott, M., Reth, A., Eggeling, L., 2012. Improved L-lysine production with *Corynebacterium glutamicum* and systemic insight into citrate synthase flux and activity. Biotechnol. Bioeng. 109 (8), 2070–2081.
Vemuri, G.N., Altman, E., Sangurdekar, D.P., Khodursky, A.B., Eiteman, M.A., 2006. Overflow metabolism in *Escherichia coli* during steady-state growth: transcriptional regulation and effect of the redox ratio. Appl. Environ. Microbiol. 72 (5), 3653–3661.
Wang, C., Liwei, M., Park, J.-B., Jeong, S.-H., Wei, G., Wang, Y., Kim, S.-W., 2018. Microbial platform for terpenoid production: *Escherichia coli* and Yeast. Front. Microbiol. 9, 1–8.
Wielgoss, S., Barrick, J.E., Tenaillon, O., Cruveiller, S., Chane-Woon-Ming, B., Medigue, C., Schneider, D., 2011. Mutation rate inferred from synonymous substitutions in a long-term evolution experiment with *Escherichia coli*. G3-Genes Genomes and Genetics 1 (3), 183–186.
Wolfe, A.J., 2005. The acetate switch. Microbiol. Mol. Biol. Rev. 69, 12–50.
Wu, X., Eiteman, M.A., 2016. Production of citramalate by metabolically engineered *Escherichia coli*. Biotechnol. Bioeng. 113 (12), 2670–2676.
Yang, J., Sun, B., Huang, H., Jiang, Y., Diao, L., Chen, B., Xu, C., Wang, X., Liu, J., Jiang, W., Yanga, S., 2014. High-efficiency scarless genetic modification in *Escherichia coli* by using lambda red recombination and I-SceI cleavage. Appl. Environ. Microbiol. 80 (13), 3826–3834.
Yang, Y.T., Bennett, G.N., San, K.Y., 2001. The effects of feed and intracellular pyruvate levels on the redistribution of metabolic fluxes in *Escherichia coli*. Metab. Eng. 3 (2), 115–123.
Zhao, J., Baba, T., Mori, H., Shimizu, K., 2004. Effect of *zwf* gene knockout on the metabolism of *Escherichia coli* grown on glucose or acetate. Metab. Eng. 6, 164–174.
Zhu, Y., Eiteman, M.A., Altman, R., Altman, E., 2008. High glycolytic plux improves pyruvate production by a metabolically engineered *Escherichia coli* strain. Appl. Environ. Microbiol. 74 (21), 6649–6655.